USCAP

ARTICLE

Sustained hedgehog signaling in medulloblastoma tumoroids is attributed to stromal astrocytes and astrocyte-derived extracellular matrix

Yan Cheng[1,2] · Janusz Franco-Barraza [ID][2] · Yuan Wang[1] · Chaonan Zheng[1] · Li Zhang[1] · Yanghui Qu[1] · Yaqiu Long[1] ·
Edna Cukierman [ID][2] · Zeng-jie Yang[2]

Abstract

Aberrant activation of the hedgehog (Hh) signaling pathway is associated with the formation of medulloblastoma (MB), the most common malignant pediatric brain tumor. However, tumor cells from human and mouse MB can not be passaged or preserved after being adherently cultured. Moreover, Hh signaling in MB cells is inactivated in such culture. Here we demonstrate that MB cells are capable of forming tumoroids (tumor spheroids) in vitro under optimized conditions, which can be further passaged and cryopreserved. More importantly, MB cells maintain Hh pathway activation and cell proliferation in tumoroids. Our studies further reveal that tumoroids-forming capacity of MB cells relies on astrocytes, a major component of the MB microenvironment. Astrocytes facilitate the formation of MB tumoroids by secreting sonic hedgehog (Shh) and generating astrocyte-derived extracellular matrix. These findings demonstrate the critical role of stromal astrocytes in supporting the survival and proliferation of MB cells in vitro. This study establishes a valid model for long-term culture of primary MB cells, which could be greatly beneficial for future investigation of MB tumorigenicity and the development of improved approaches to treat MB.

Introduction

Hedgehog (Hh) signaling plays a critical role in the normal mammalian development in mammalian cells [1]. In brief, Hh ligands bind to Patched (Ptch1), resulting in the internalization and degradation of Ptch1, thereby releasing Smoothened (Smo) to enter the primary cilia. Smo in the cilia promotes dissociation of glioma-associated oncogene homolog (Gli) from Suppressor-of-fused (Sufu), causing

nuclear translocation and activation of Gli1 and Gli2 transcription factors, as well as the degradation of Gli3, an inhibitory Gli protein [2, 3]. Activating mutations in the Hh pathway drive known human malignancies including medulloblastoma (MB) and basal cell carcinoma. MB is the most common malignant brain tumor in children, which arises in developing cerebellum, and grows rapidly spreading through the CNS. According to current consensus, there are at least four molecular subgroups of MB, including Hedgehog (Hh), WNT, group 3 and 4 [4]. Hh-MB accounts for ~30% cases of Human MB cases.

We previously reported that astrocytes, a major component of MB microenvironment, supported Hh signaling as well as the proliferation of tumor cells [5]. Astrocytes secreted the sonic hedgehog (Shh) ligand, which induced MB cells to express Nestin, an intermediate filament protein. Nestin plays an important role in MB progression through abolishing the inhibitory functions of Gli3 to fuel Hh signaling [6].

Hh signaling is known to induce the proliferation/activation of stromal cells that account for the majority of the extracellular matrix (ECM) in a tumor mass [7, 8]. The ECM is commonly defined as the non-cellular component of tissue that provides both biochemical and structural support to local cells [9]. The

✉ Edna Cukierman
edna.cukierman@fccc.edu

✉ Zeng-jie Yang
zengjie.yang@fccc.edu

1   College of Pharmaceutical Sciences, Soochow University, Suzhou, China

2   Cancer biology program, Fox Chase Cancer Center, Temple University Health System, Philadelphia, PA, USA

ECM is a key component of the tumor microenvironment and it is known to be important for tumor initiation, progression, and metastasis [10]. Integrins are the main cell-ECM adhesion receptors, composed of non-covalently linked heterodimers (e.g., one α and one β glycoprotein subunits), which detect changes in the physical structure of ECM protein polymers/ligands, like fibronectin and collagen, known to play important roles in the tumorigenesis [11, 12].

So far, there are three FDA-approved Hh pathway inhibitors including vismodegib, sonidegib, and glasdegib. However, due to toxicities as well as the drug resistance, these inhibitors are not currently applied for MB treatment. Thus, there is a great demand for developing effective Hh pathway inhibitors for MB treatment. However, the development of Hh pathway inhibitors is being significantly impeded by lack of tumor cell lines with the activation of Hh pathway. Approximately 15% of mice with heterozygous *Patched1* (*Ptch1*) mutation (*Ptch1* ± mice) develop tumors in their cerebella resembling the Hh group MB in human [13]. Conditional deletion of *Ptch1* in cerebellar granule neuron precursors (GNPs) in *Math1-Cre/Ptch1^fl/fl* mice caused MB formation with 100% penetrance [14]. Tumor cells from *Ptch1* mutant mice exhibit an activated Hh pathway. However, all previous attempts to generate a murine MB cell line that retain Hh pathway activity in vitro failed [15]. Although tumor cells from the above MB models can be readily purified and cultured, they do not sustain Hh signaling in vitro [15, 16]. In addition, these primary MB cells tend to differentiate in vitro, which negates the possibility to passage or preserve the MB cell lines. The above-listed limitations greatly preclude the utilization of these primary MB cells in the basic research and preclinical studies of MB.

Here we demonstrated that MB cells from *Ptch1* mutant mice can be cultured in vitro as tumoroids (i.e., tumor spheroids) that sustain activation of the Hh pathway. Primary MB cells in tumoroids can be passaged and preserved, allowing the long-term maintenance and storage of tumor cells. Moreover, MB cells in tumoroids retained their tumorigenicity. We further revealed that sustained Hh signaling in tumoroids relied on the Shh ligand and the ECM that was produced by astrocytes; removal of astrocytes or blockage of Shh secretion from astrocytes markedly inhibited the formation of tumoroids from MB cells. Our studies established a feasible approach to culture primary MB cell retaining Hh signaling and tumorigenicity.

Materials and methods

Mice

Ptch1^fl/fl mice, *Math1-Cre* Mice, *Ptch1-lacZ* mice, Wild type mice, *Cas9* mice, and *R26R-GFP* mice were from the Jackson Laboratory. *CB17/SCID* mice were purchased from the Laboratory Animal Facility (LAF) at Fox Chase Cancer Center.

All animals were maintained in the LAF at Fox Chase Cancer Center, and all experiments were performed in accordance with procedures approved by the Fox Chase Cancer Center Animal Care and Use Committee.

Cell isolation, flow cytometry, and lentivirus preparation

In this study, unless mentioned otherwise, all MB cells were isolated from *Math1-Cre/Ptch1^fl/fl* mice at 8 weeks of age as previously described [17]. Primary MB cells were isolated from mouse cerebella using papain dissociation buffer, containing 10 U/ml papain (Worthington), 200 μg/ml L-cysteine (Sigma), and 250 U/ml DNase (Sigma). The cell suspension was filtered (70 μm) and re-suspended in designated culture media for tumoroid formation. For purifying astrocytes and tumor cells from *Math1-Cre/Ptch1^fl/fl/Rosa-GFP* mice or isolating astrocytes from wild type cerebella at postnatal day 1–2, tumor tissues or cerebella were dissociated as mentioned above, and the cell suspension was immunostained with an APC-conjugated antibody against ACSA2 (astrocyte cell surface antigen 2) for 30 min. Tumor cells (GFP+) and astrocytes (APC+) were harvested by FACs as previously described [5].

Lentiviruses were produced by transfecting HEK293T cells with the pFUGW vector expressing GFP and helper plasmids (pMD2G and psPAX2) according to the standard procedure.

Shh supernatant was generated by transfecting HEK293T cells with Shh-N expression plasmid (David Robbins, Dartmouth Medical School, Hanover, NH) and harvesting the supernatant for 3 days. The supernatant was used at 30% for MB cells.

MB cell culture in vitro

For adherent cell culture

MB cells were plated on poly-D-lysine (PDL) coated coverslips (12 mm, Biosciences) at a density of $2–4 \times 10^5$ cells/coverslip or into a 24-well plate at a density of $1–2 \times 10^6$ cells/well. Cells were maintained in NB-B27 medium containing Neurobasal medium with B27 supplement (NB-B27, Washington), 1 mmol/L sodium pyruvate, 2 mmol/L L-glutamine, and 1% Pen/Strep.

For tumoroid culture

MB cells were cultured in 6-well plate (2×10^5 cells/well) using different culture media including NB-B27 medium

plus 1% fetal bovine serum (FBS, Hyclone); NB-B27 medium plus 3% FBS; Neurocult basal medium (Stem Cell Technologies) with 10 ng/ml FGF and 20 ng/ml EGF; or DMEM with 10% FBS. In some experiments, cells were dissociated from tumor spheroids using Accutase (Sigma) and passaged every 4 days. For counting the number of tumoroids, 50 μl of tumoroids suspension were collected and the number of tumoroids was counted under a microscope. Established tumoroids were defined by a minimal sphere size spanning at least 50 μm in diameter.

For Trypan Blue exclusion analysis to examine the survival of tumor cells, tumoroids were dissociated and resuspended in a 0.4% Trypan Blue solution. Non-viable (blue) and viable cells (unstained) were counted using a hemocytometer.

Intracranial transplantation

Cells isolated from tumoroids were injected into the cerebella of *CB17/SCID* mice (at 6–8 weeks of age) using a stereotaxic apparatus (Kopf, Tujunda, CA) as previously described [17]. 1×10^6 cells were injected into each recipient mouse cerebellum. Note that cells after adherently cultured were harvested by centrifugation at 300 g to remove dead cells and cellular debris.

Extracellular matrix preparation

To prepare astrocyte-derived ECM, we used our well-established fibroblast/mesenchymal cell-derived ECM method [18, 19]. Briefly, astrocytes isolated from mouse cerebella at postnatal day 1, were plated onto 24-well plates that were pre-coated with 0.2% gelatin. Astrocytes were cultured for 12 h with DMEM plus 10% fetal bovine serum. This matrix medium was replaced daily with fresh matrix medium containing 75–150 μg/ml ascorbic acid. After 7–9 days, astrocytes were removed, leaving acellular ECM intact using an extraction buffer (1X DPBS with 0.5% Triton X-100, 20 mM NH$_4$OH). The remaining astrocyte-derived ECM was further washed with DPBS and treated with DNase I. In some experiments, MB cells were plated into astrocyte-derived ECMs at a density of 2×10^6 cells/ECM-well (in a 24-well plate configuration).

Immunohistochemistry

For immunofluorescence analyses, tumoroids or tumor sections were collected and fixed with 4% paraformaldehyde (PFA). After permeabilization with PBS containing 0.1% Triton X-100, tumoroids or tumor sections were blocked for 1 h with Odyssey Blocking Buffer (LI-COR Biosciences, NE), followed by incubation with primary antibodies overnight at 4 °C, and then with secondary antibodies for 2 h at room temperature. Tumoroids or tissue sections were counterstained with DAPI and mounted with Fluoromount G (Southern Biotechnology).

In some experiments, tumor cells were pulsed with BrdU or EdU (10 μM, Millipore) for 2 h prior to harvesting. After fixing in 4% PFA, cells were treated with DNase Buffer (4.2 mM MgCl2, 0.15 M NaCl, 50 U DNase, PH 5.0) or EdU staining solution(100 mM Tris, 1 mM CuSO$_4$, 10 μM Fluorescent Azide, 100 mM Ascorbic acid) at 37 °C for 30 min before immunofluorescence analysis of BrdU/EdU incorporation following the standard protocol [20].

Primary antibodies used in this study were: anti-Ki67 (1:500, Abcam), anti-MAP2 (1:500, Abcam), anti-cleaved caspase3 (1:500, Cell Signaling Technology), anti-βIII-tubulin (1:500, Abcam), anti-Zic1 (1:500, BD), anti-GFP (1:500, Invitrogen), anti-S100β (1:500, Sigma), anti-BLBP (1:500, Millipore), anti-AN2-PE (1:100, Miltenyi Biotec), anti-CD68-PE (1:100, Miltenyi Biotec), anti-Pax6 (1:500, Millipore), anti-ACSA2-APC (1:100, Miltenyi Biotec), anti-Nestin (1:1,000, Abcam), anti-Shh (1:1000, Cell Signaling Technology), anti-fibronectin (1:500, Sigma), anti-BrdU (1:500, Sigma), anti-GFAP (1:500, Millipore), and anti-synaptophysin (1:500, Abcam).

qPCR

Total RNA was extracted from MB cells by Trizol reagent (Sigma-Aldrich). cDNA was synthesized by using a Qiagen RT kit according to the supplier's protocol. mRNA expression levels were examined by Bio-Rad iQ SYBR Green Supermix (Bio-Rad) and the Bio-Rad iQ5 Multicolor Real-Time PCR Detection System. Data were normalized to endogenous glyceradehyde-3-phosphate dehydrogenase for each sample. Primer sequences are available upon request. Sequences of guide RNAs for Shh deletion: sg1, ACCTTCCTGGA CCGCGACGA; sg2, TGGCGCCGCA CAACGACTCG.

Integrin inhibition assay

The integrin inhibition experiments were performed as previously described [19]. Freshly isolated MB cells were resuspended in NB-B27 medium and incubated with the following anti-integrins antibodies or isotype controls for 30 min before being plated on PDL-coated coverslips or into astrocyte-derived ECMs. After being cultured 24 h, tumor cells were treated daily with the functional antibodies for 2 more days. All functional antibodies and isotype controls were Azide free and used at final concentration of 10 μg/ml. These included: anti-murine Integrin β1 (clone AIIB2, MABT409, Sigma-Aldrich) and its IgG1 murine isotype control (clone HRPN, MABF1786, Sigma-Aldrich), anti-murine Integrin α5β1 (BMA5, MAB1984-I, Sigma-Aldrich)
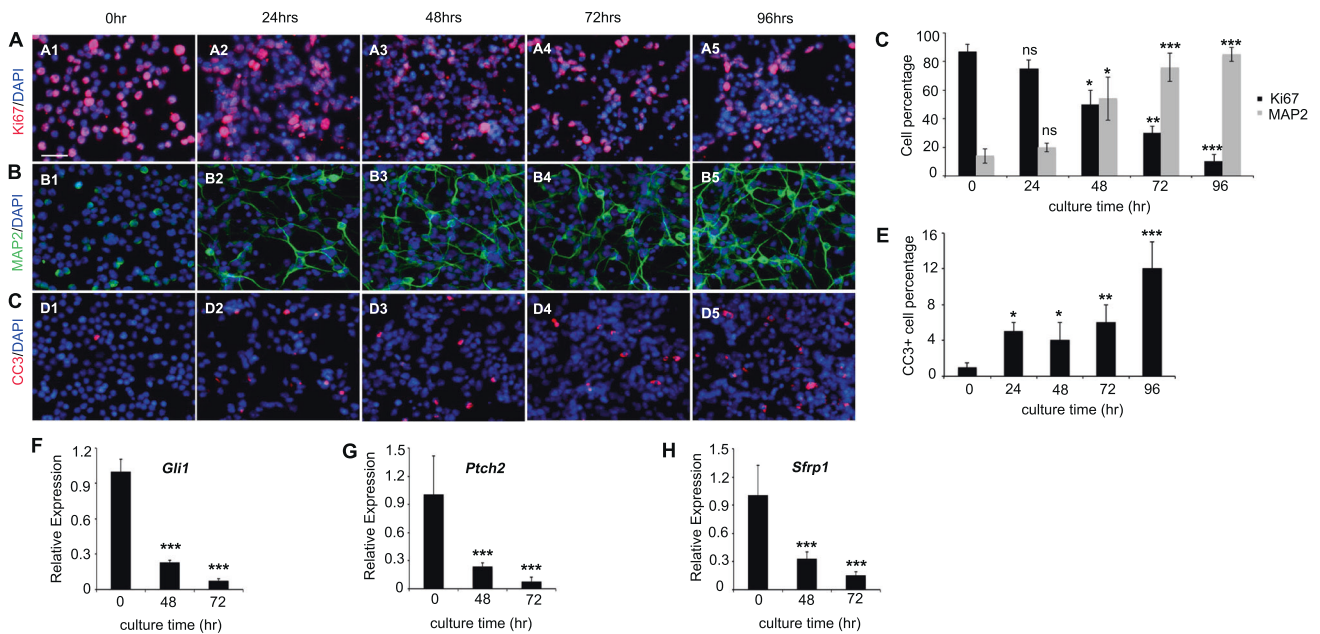
Fig. 1 Hh signaling is inactivated in adherently cultured MB cells. Primary MB cells isolated from *Math1-Cre/ptch1^{fl/fl}* mice, were plated under the adherent culturing conditions (on PDL-coated coverslips) for the denoted time periods. **a–c** Indirect immunofluorescence of adherent MB cultures showing the expression of Ki67 (**A1–A5**) and MAP2 (**B1–B5**). Percentages of Ki67+ cells and MAP2+ cells in adherent cultures at denoted timepoints as shown in the graph (**c**). DAPI was used to counterstain cell nuclei. **d, e** The time-course examination of cleaved caspase3 (CC3) in cultured MB cells showing indirect immunofluorescent representative images (**D1–D5**), and corresponding percentage of cells positive for CC3 (**e**). **f–h** Expression of *Gli1*, *Ptch2*, and *Sfrp1* mRNA in adherently cultured MB cells examined by q-PCR. Scale bar: 50 μm.

and IgG2b Negative Control (clone LTF-2, MABF1076Z, Sigma-Aldrich), as well as recombinant anti-murine Integrin αv (low endotoxin EPR16800, ab222222, Abcam) and recombinant rabbit IgG isotype control (EPR25A, ab172730, Abcam).

Collagen fiber assessment; second harmonic generation (SHG) of polarized light microscopy and digital image analysis

Astrocyte-derived ECMs were deposited on glass coverslips, fixed with 4% PFA and mounted using Fluoromount-G. To acquire SHG indicative of polymerized/fibrillar collagen, a Leica SP8 DIVE confocal/multiphoton microscope system (Leica, Germany) was used. Specimens were imaged with a 25X HC FLUOTAR L 25×/0.95NA W VISIR water-immersion objective and excited at 850 nm with IR laser Chameleon Vision II (Coherent, CA). Backward SHG emission was collected using a non-descanned detector configured to register wavelengths between 410–440 nm. Specimens from astrocytes isolated from three different animals, per phenotype, were assessed. An average of five fields per coverslip, ($n = 15$ images per phenotype), were scanned using identical settings and recorded as monochromatic, 16-bit image stacks set to an average of 20 μm Z distances, using the Leica Application Suite X 3.5.5 software.

Digital imaging analyses were conducted via FIJI (ImageJ 1.52p). Raw image stacks were three-dimensional reconstituted as maximum projections preserving original SHG intensities. Signal to noise thresholds were set identically for images from each experimental repetition. Positive signal areas were used to calculate integrated SHG intensities (e.g., SHG signal/SHG area) as integrated density. Control mean integrated intensity values were used for data normalization; results are expressed as arbitrary units compared with the control.

Statistical analysis

Student's *t* test was performed to determine the statistically significant differences using means and comparing experimental samples to controls (e.g., 0 h, or DMSO treatment, etc.). *, $p < 0.05$; **, $p < 0.01$; ***, $p < 0.001$; ns, not significant. $p < 0.05$ was considered statistically significant. Error bars shown in figures represent SEM from at least three independent experiments. Difference in the survival of *CB17/SCID* mice after cell transplantation was assessed using the Kaplan–Meier survival analysis and the mantel–Cox log-rank test was used to assess the significance of difference between two cohorts of tumor bearing mice. Data handling and statistical processing was performed using Microsoft Excel and Graphpad Prism Software.
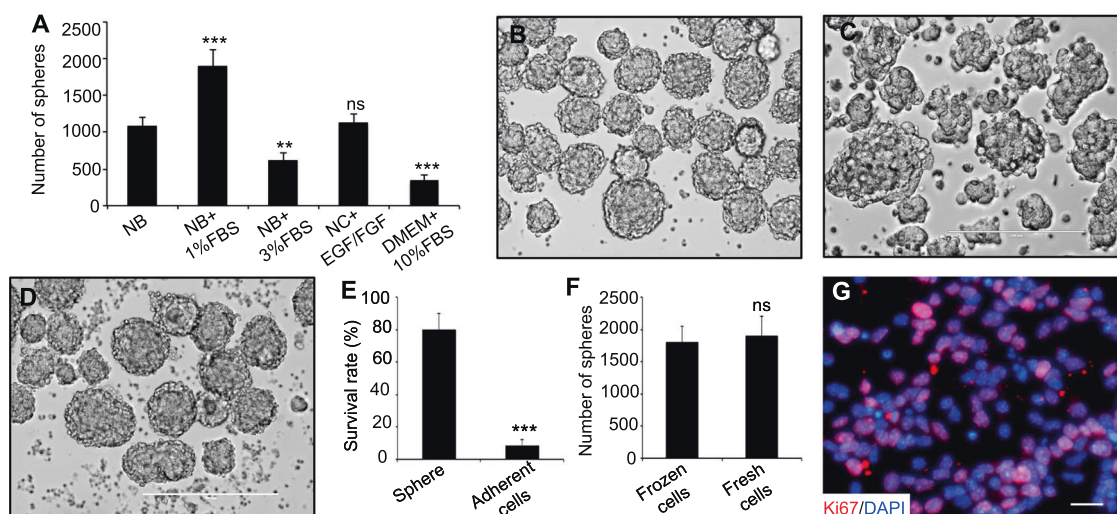
Fig. 2 MB cells form three-dimensional tumoroids in vitro. a, **b** Primary MB cells, isolated from *Math1-Cre/Ptch1*^*fl/fl* mice, were cultured in suspension for 4 days using assorted media and tumoroid numbers are shown (**a**). A bright-field image of tumoroids generated in the presence of NB-B27/1% serum (**b**). **c** A bright-field image of tumoroids from human Hh-MB cells using NB-B27/1% serum. **d** A bright-field image of tumoroids regenerated from cells dissociated from initiating tumoroids. **e** The viability of cells dissociated from tumoroids and those from adherent cell culture by Trypan Blue exclusion assay. **f** The number of tumoroids derived from identical numbers of cells dissociated from cryopreserved tumoroids, and from freshly isolated MB cells. **g** Tumor cells from cryopreserved tumoroids were immunostained for Ki67 following dissociation and initial adherent plating. DAPI was used to counterstain cell nuclei. Scale bars: 200 μm (**b**–**d**), 50 μm (**g**).

Results

Hedgehog signaling in MB cells is inactivated under adherent culture conditions

MB cells isolated from *Math1-Cre/Ptch1*^*fl/fl* mice at 8 weeks of age, were plated on PDL-coated coverslips, with NB-B27 culture medium as previously described [6]. Tumor cells were harvested at different timepoints, to examine their proliferation, differentiation, and survival by immunocytochemistry. As shown in Fig. 1 (panel A1), MB cells were highly proliferative at time of isolation, when first plated (0 h), with more than 90% of tumor cells staining positive for Ki67. However, tumor cells gradually exit the cell cycle, evidenced by progressively decreased percentage in numbers of proliferating cells (Ki67+) (Fig. 1 panels A2–A4). By 96 h, <20% of tumor cells were Ki67+ (Fig. 1 panel A5). At 0 h, right after being plated, ~14% of tumor cells expressed the microtubule associated protein 2 (MAP2) (Fig. 1 panel B1), an established marker for neuronal differentiation [21], suggesting that a small proportion of isolated cells was differentiated in the initial culture. An increasing number of tumor cells started to expressing MAP2 after being cultured (Fig. 1 panels B2–B5). At 96 h, over 85% of tumor cells were MAP2+, and the majority of tumor cells exhibited a bipolar morphology (Fig. 1 panel B5), indicating that majority of tumor cells proceeded to differentiate in vitro. The above changes in the percentage of Ki67+ cells and MAP2+ cells (Fig. 1c), suggests that

adherently cultured MB cells autonomously cease their proliferation and initiate differentiation. The in vitro differentiation of MB cells in the adherent culture was also confirmed by the expression of βIII-tubulin, another established marker for neuronal differentiation [22] (supplementary Fig. S1). In addition, we evaluated tumor cell survival in culture by immunostaining for cleaved caspase-3 (CC3). The percentage of CC3+ cells was gradually increased among MB cells in the adherent culture (Fig. 1 panel D1–D5 and Fig. 1e). These data suggest that the survival of MB cells is progressively compromised in adherent culture. In addition, the percentage of tumor stromal cells including astrocytes (S100β+), microglia (CD68+) as well as oligodendrocytes precursor cells (NG2+) was significantly reduced in adherent tumor cell culture compared with that immediately following isolation (supplementary Fig. S2), suggesting that the adherent culture condition does not support the amplification of these types of stromal cells.

To assess Hh signaling, we examined the expression of Hh pathway target genes including *Gli1*, *Ptch2*, and *Sfrp1* in the adherently cultured MB cells via q-PCR. As shown in Fig. 1f–h, despite significant levels of all three transcripts initially detected (e.g., at 0 h), the levels of all three transcripts significantly declined in time. These data suggest that Hh signaling was repressed in MB cells in adherent culture. To determine whether the repressed Hh signaling in MB cells was due to the incomplete *Ptch1* deletion, we examined the presence of the *Ptch1* gene in tumor cells. The
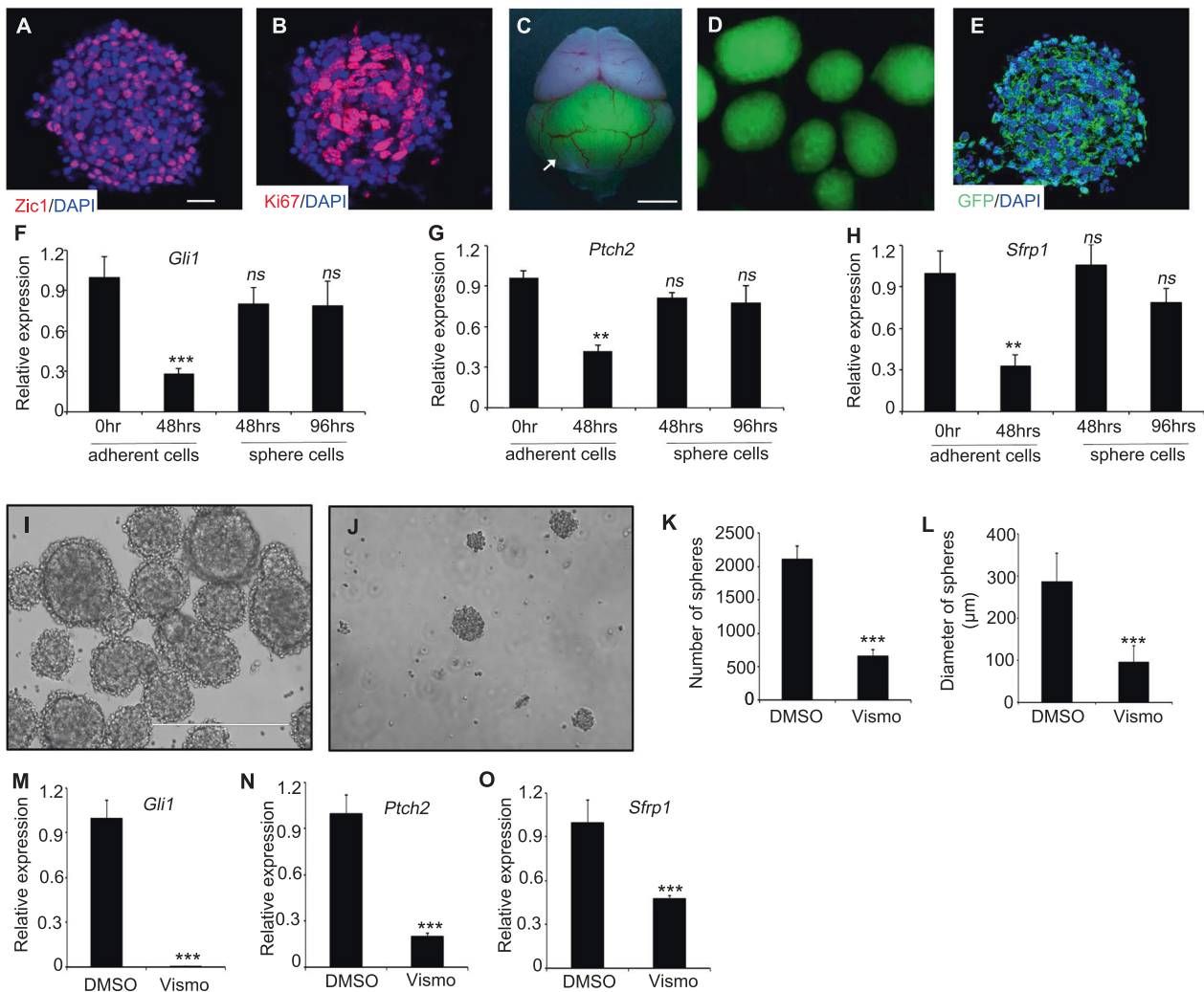
Fig. 3 Hh signaling is sustained in MB cells in tumoroids. a, b Tumoroids were collected to examine Zic1 protein (**a**) and Ki67 protein (**b**) by immunofluorescence. DAPI was used to counterstain cell nuclei. **c** A whole-mount brain image from a *Math1-Cre/Ptch1^{fl/fl}/R26R-GFP* mouse at 8 weeks of age. **d, e** GFP signal from tumoroids formed by MB cells from a *Math1-Cre/Ptch1^{fl/fl}/R26R-GFP* mouse (**d**) Tumoroids were harvested for immunocytochemistry to examine GFP expression (**e**). **f–h** Expression of *Gli1* (**f**), *Ptch2* (**g**), or *Sfrp1* (**h**) mRNAs in MB cells freshly isolated from *Math1-Cre/Ptch1^{fl/fl}* mice (0 h), MB cells adherently cultured for 48 h (adherent cells) and tumoroids (sphere cells) formed at 48 h or 96 h in culture, examined by q-PCR. **i–n** MB tumoroids were cultured for 4 days under tumoroid condition in the presence of DMSO (**i**) or 200 nM vismodegib (**j**). The number and size (in diameter) of tumoroids in culture was quantified in (**k**) and (**l**), respectively. After the treatment, tumoroids were harvested to examine mRNA expression of *Gli1* (**m**), *Ptch2* (**n**) or *Sfrp1* (**o**) by q-PCR. Scale bars: 50 μm (**a, b, d, e**); 200 μm (**i, j**).

exon 3 in *Ptch1* gene that is flanked by loxp sites, is deleted in tumor cells from *Math1-Cre/Ptch1^{fl/fl}* mice; whereas exon 14 of *Ptch1* gene remains intact in tumor cells [14, 23]. Therefore, the absence of *Ptch1* exon 3 in genomic DNA, relative to the presence of the exon 14, directly correlates with the extent of *Ptch1* deletion in tumor cells of these mice. As shown in supplementary Fig. S3, while both exons were readily detected in the genomic DNA from control GNPs, exon 3 of *Ptch1* gene was almost completely missing from the DNA in MB cell. The significantly weaker band of PCR product from exon 3 of *Ptch1* that was still detected from MB cells based on the DNA electrophoresis, could be derived from the few stromal cells contaminants.

Collectively, the above data confirm that MB cells failed to sustain the proliferation and Hh signaling under adherent culturing conditions.

MB cells form three-dimensional tumoroids upon culturing in suspension

Recent studies reveal that tumoroids (i.e., spheroids of tumor cells) recapitulate important in vivo pathological features of tumor cells [24, 25]. To establish a method for maintaining Hh signaling in MB cells, we examined whether MB cells can form three-dimensional tumoroids in vitro. MB cells isolated from *Math1-Cre/Ptch1^{fl/fl}* mice at

8 weeks of age, were suspended in assorted media including NB-B27/1% FBS; NB-B27/3%FBS; Neurocult/EGF + FGF (the medium often used to culture stem cells); and DMEM/10%FBS (the conventional medium used for culturing cell lines). NB-B27 was tested as it is known to support neuronal survival and functions in vitro [26]. Following 4 days in non-adherent culture (in suspension), tumoroids were harvested and sphere appearances and numbers were gauged. As shown in Fig. 2a, tumoroids were found in the culture under all tested conditions, demonstrating the ability of MB cells to form tumroids in vitro. The number of tumoroids was significantly reduced in the culture with NB-B27/3%FBS and DMEM/10%FBS, compared with that in the medium containing NB-B27 alone, implying that high serum concentration may restrict tumoroid formation. The most abundant tumoroids were detected in the culture with NB-B27/1% FBS (Fig. 2a, b), hence representing the most optimal conditions for MB tumoroid formation. In addition, human MB cells (Hh group, ICb-5610MB) also formed tumoroids in the presence of NB-B27/1% FBS (Fig. 2c). Hence, NB-B27/1% FBS was used for tumoroid formation in the rest of this study.

We next examined whether MB tumoroids can be passaged in culture. MB cells from *Math1-Cre/Ptch1^{fl/fl}* mice at 8 weeks of age, were cultured in suspension for 4 days to form tumoroids, which were then dissociated and resuspended in NB-B27/1% FBS for four additional days. As shown in Fig. 2d, tumoroids, resembling the original ones, were re-generated from the cells that were dissociated from the initial tumoroids. We then assessed the viability of tumor cells isolated from tumoroids by Trypan Blue exclusion analysis. MB cells adherently cultured for 4 days were used as a control. Over 80% of cells dissociated from tumoroids were alive (Fig. 2e). As a comparison, more than 90% of adherent MB cells were no longer viable, partially due to mechanical damages of differentiated tumor cells (with long processes) during cell harvesting. Tumoroids can be passaged for at least five times, with no observed alterations in cell survival and sphere-forming capacity of tumor cells (data not shown). These data indicate that tumoroids constitute an assertive approach for culturing and maintaining MB cells in vitro.

To test whether MB tumoroids could be cryopreserved, we suspended MB tumoroids in a cryopreservation solution consisting of 10% DMSO plus 90% fetal bovine serum, which were stored at −80 °C for 2 months. After thawing, tumoroids were dissociated and tested for their ability to re-form tumoroids. MB cells freshly isolated from *Math1-Cre/Ptch1^{fl/fl}* mice were also cultured for tumoroid formation as a control. As shown in Fig. 2f, a comparable number of tumoroids was observed among tumor cells from frozen tumoroids and freshly isolated MB cells. These data suggest that tumoroid-forming capacity of MB cells was not

significantly compromised by the cryopreservation. In addition, MB cells dissociated from frozen tumoroids were adherently cultured on PDL-coated coverslips. Similar to freshly isolated MB cells (as shown in Fig. 1a), the majority of tumor cells (>90%) attached to the coverslips and resumed the proliferation (Ki67+, Fig. 2g). These findings indicate that MB cells can be preserved as frozen tumoroids.

MB tumoroids sustain Hh signaling in tumoroids

We further characterized tumoroids via immunocytochemistry. As expected, tumor cells in tumoroids expressed high levels of Zic1 (Fig. 3a), an established marker for MB cells [27], suggesting that tumoroids were dominated by MB cells. Ki67 expression was also detected in the majority of tumoroids cells (Fig. 3b), indicating that these were enriched with proliferative cells. Multipotent neural stem cells (NSCs) in the brain can form tumoroids in vitro [28]. To confirm tumoroids originated from MB cells as opposed to normal NSCs present in tumor tissues, we utilized *Math1-Cre/Ptch1^{fl/fl}/R26R-GFP* mice, in which MB cells permanently express GFP [14, 29]. GFP fluorescence was readily detected in the MB tissue developed from *Math1-Cre/Ptch1^{fl/fl}/R26R-GFP* mice (Fig. 3c). MB cells isolated from the *Math1-Cre/Ptch1^{fl/fl}/R26R-GFP* mice were cultured to obtain tumoroids. As shown in Fig. 3d, all tumoroids exhibited intensive GFP fluorescence. Moreover, the majority of cells in tumoroids were GFP positive for GFP by immunocytochemistry (Fig. 3e). These data suggest that tumoroids generated by this method, are predominately composed of MB cells.

We then investigated Hh signaling in tumoroids by examining the expression of Hh pathway target genes including *Gli1*, *Ptch2*, and *Sfrp1*, in MB cells cultured in tumoroids for 48 h or 96 h. MB cells freshly isolated (0 h) or adherently cultured for 48 h, were harvested as controls. As expected, the expression of all three Hh pathway genes was significantly down-regulated in MB cells after 48 h in adherent culture (Fig. 3f–h). Notably, high levels of *Gli1*, *Ptch2*, and *Sfrp1* expression were detected and sustained in the tumoroids (Fig. 3f–h). These data suggest that Hh signaling is indeed maintained by MB cells cultured as tumoroids. To further confirm the activation of Hh pathway in tumoroids, we tested whether tumoroids formation can be inhibited by vismodegib, a potent antagonist of Smoothened [30]. MB cells were cultured under tumoroids condition in NB-B27/1%FBS containing vismodegib (200 nM) or DMSO as a vehicle control. As expected, MB cells readily formed tumoroids in the control culture, whereas the number of tumoroids was markedly reduced in MB cell cultured with vismodegib (Fig. 3i–k). In addition, the size of tumor tumoroids was also decreased following the treatment with vismodegib (Fig. 3l). These data suggest that tumoroid
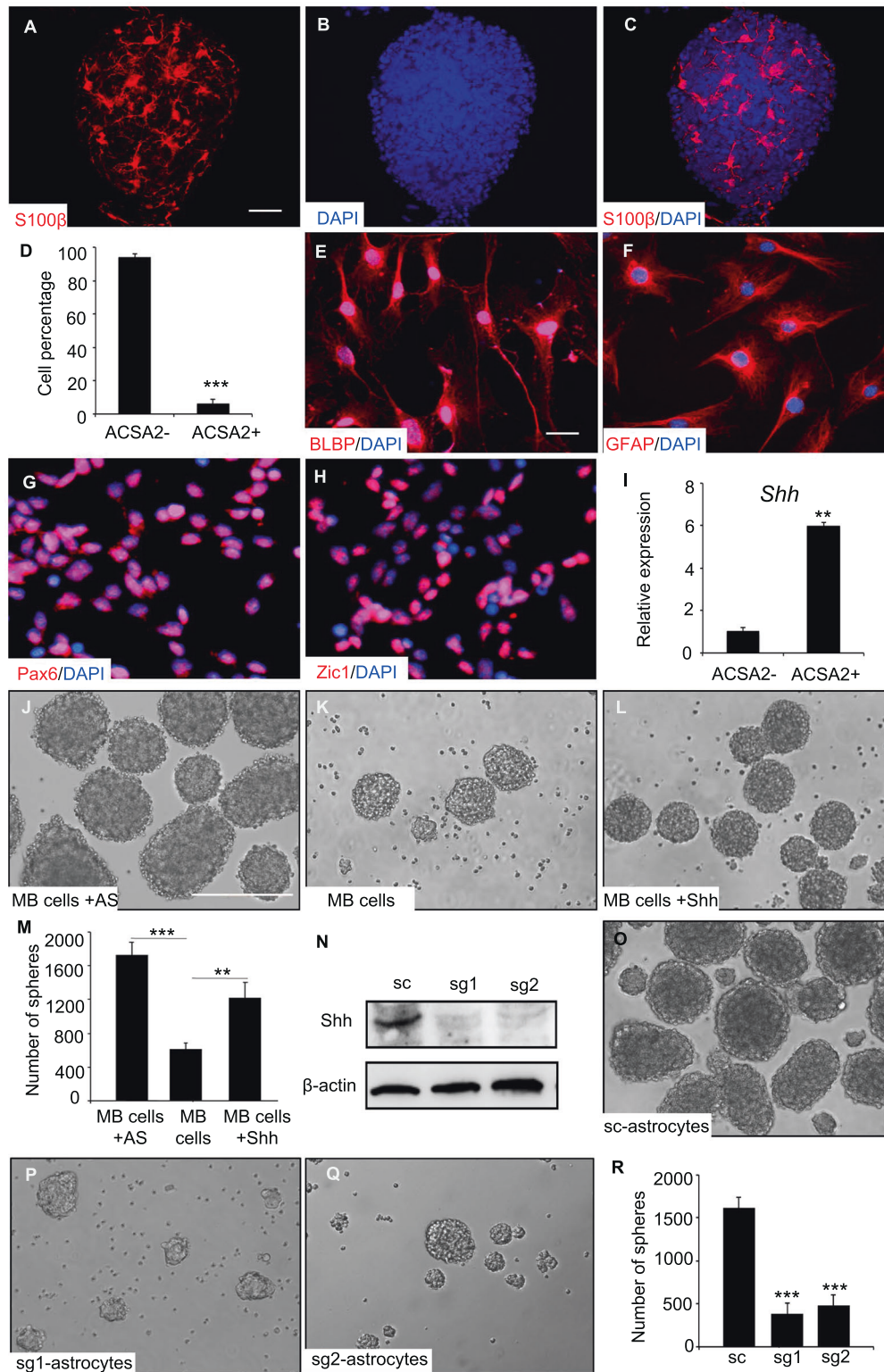
formation of MB cells relies on Hh signaling. We then harvested tumoroids after treatment with vismodegib or DMSO, and examined the expression of *Gli1*, *Ptch2*, and *Sfrp1* in tumoroid cells by q-PCR. As shown in Fig. 3m–o, the expression of all three transcripts was significantly down-regulated in tumoroids treated with vismodegib compared with vehicle control (DMSO), suggesting that Hh signaling in tumoroids was indeed inhibited by vismodegib

◀ **Fig. 4 Astrocyte-derived Shh is necessary for MB tumoroid formation. a–c** Tumoroids were harvested to examine S100β by indirect immunofluorescence (**a**). DAPI was used to counterstain cell nuclei (**b**). A merged image showing S100β expression and DAPI staining in a selected tumoroid (**c**). **d–i** Percentage of ACSA2+ cells and ACSA2- cells in tumoroids based on flow cytometry (**d**). ACSA2+ cells were plated and examined BLBP (**e**) and GFAP (**f**) by indirect immuno-fluorescence. ACSA2- cells were examined for the expression of Pax6 (**g**) and Zic1 (**h**) indirect immunofluorescence. Shh mRNA expression in ACSA2+ cells, relative to that in ACSA2- cells (**i**). **j–m** Purified MB cells (ACSA2-) alone (**j**), together with astrocytes (ACSA2+) (**k**) or alone treated with Shh conditioned media (**l**) were cultured for 4 days. The number of tumoroids in (**j**), (**k**) and (**l**) was quantified and graphed (**m**). **n–q** Astrocytes from Cas-9 mice were infected with lentivirus carrying scrambled RNA (sc) or guide RNA specific for Shh (sg1, sg2). 48 h following the infection, astrocytes were harvested to examine Shh protein expression by western blotting. β-actin was used as a load control (**n**). Tumoroid formation in MB cells co-cultured with control astrocytes (**o**, infected with scrambled RNA) or with Shh-deficient astrocytes (sg1, **p**; sg2, **q**). The number of tumoroids in the presence of astrocytes was quantified (**r**). Scale bars: 50 μm (**a–c**), 20 μm (**e–h**), 200 μm (**j–l**, **o–q**).

treatment. Together, these data demonstrate that Hh pathway is activated in the ex vivo three-dimensional MB tumoroids.

NB-B27 plus 1% FBS represents the most optimal medium supporting the formation of tumoroids, we then examined whether the same medium (instead of NB-B27 alone) can sustain Hh signaling in MB cells in adherent culture. We cultured MB cells on PDL-coated coverslips with NB-B27 in the presence/absence of 1% FBS. After being cultured for 48 h or 72 h, MB cells were harvested to examine Hh signaling. As shown in supplementary Fig. S4, Hh signaling was gradually diminished in MB cells cultured with NB-B27 in the absence or presence of 1% FBS. These data suggest that compromised Hh signaling in adherent MB cells is not due to the lack of 1% FBS in the culture medium.

Astrocyte-derived Shh promotes MB tumoroid formation

Having observed the constitutive activation of Hh pathway in MB tumoroids, we next sought to investigate the mechanisms for MB cells to maintain Hh signaling in the tumoroids. Our previous studies demonstrated that astrocytes support the proliferation as well as Hh signaling of MB cells via secretion of Shh ligand [5]. This led us to examine the presence of astrocytes (and other stromal components) in MB tumoroids. For this purpose, tumoroids were prepared and analyzed via immunofluoresnce. As shown in Fig. 4a–c as well as in the supplementary Fig. S5, a significant amount of tumoroid cells stained positive for two established markers for astrocytes, S100β and brain lipid-binding protein (BLBP) [31]. To further characterize

astrocytes in tumoroids, we dissociated the MB tumoroids and purified astrocytes by FACs using an antibody against Astrocytes Cell Surface Antigen 2 (ACSA2), a surface marker for astrocytes, as previously described [5]. Approximately 6% of cells in MB tumoroids were identified as ACSA2+ (Fig. 4d). ACSA2+ and ACSA2- cell populations were collected and plated them in vitro for an additional indirect immunofluorescence analysis. As shown in Fig. 4e, f, the isolated ACSA2+ cells also expressed GFAP and BLBP, two established astrocyte markers [32]. In comparison, almost all ACSA2- cells expressed Pax6 and Zic1 (Fig. 4g, h), known MB cell markers [33], indicating that ACSA2- cells were enriched with tumor cells and accounted for the majority of cells in the tumoroids. We then examined Shh mRNA expression in astrocytes (ACSA2+) and in the tumor cells (ACSA2-) isolated from the intial tumoroids. Elevated expression levels of Shh mRNA were detected in astrocytes compared with tumor cells (Fig. 4i), in agreement with our previous report [5]. In addition, flow cytometry further revealed that besides astrocytes, a small number of other stromal cells was included in MB tumoroids. These were indentified as endothelial cells (CD31+, $1.64 \pm 0.12\%$), microglia (CD68+, $1.29 \pm 0.83\%$) and oligodendrocyte precursor cells (OPCs, NG2+, $2.39 \pm 0.45\%$) were found in MB tumoroids. However, no immune cells (CD45+) or purkinje neurons (Calbindin+) were detected in MB tumoroids (data not shown).

To examine whether astrocytes are necessary for tumor cells to form MB tumoroids, we evaluated tumoroid-forming capacity of MB cells in the presence/absence of astrocytes. MB cells from *Math1-Cre/Ptch1fl/fl* mice were fractionated into astrocytes (ACSA2+) and tumor cells (ACSA2-) by FACS. Tumor cells together with astrocytes (the number of tumor cells/astrocytes=10:1) were co-cultured in suspension to test the ability to reconstitute three-dimensional tumoroids. Tumor cells were also cultured alone in the presence or absence of 30% Shh supernatant (obtained from the conditioned medium of 293 cells [34]). Tumoroids were readily formed in the culture of MB cells with astrocytes (Fig. 4j). Only a small number of tumoroids were detected from MB cell monocultures (Fig. 4k), whereas the number of tumoroids increased significantly (but not to the levels of the co-cultures) in the presence of Shh (Fig. 4l, m). These data further confirm the role of astrocytes and secreted Shh in supporting the formation of MB tumoroids.

To determine whether Shh from astrocytes is critical for tumoroid formation of MB cells, we isolated astrocytes from CRISPR/Cas9 knock-in mice at postnatal day 2 [35]. Astrocytes were then infected with a lentivirus carrying guide RNAs specific for Shh gene (sg1 or sg2), or a scrambled RNA (sc) as a control. Astrocytes were harvested

at 48 h following the infection and examined for efficiency of Shh deletion by western blotting. As shown in Fig. 4n, the levels of Shh protein were markedly declined in astrocytes following the infection with guide RNAs (sg1 or sg2) compared with control astrocytes. Infected astrocytes were then co-cultured with purified MB cells for testing the ability to induce MB tumoroids formation. As expected, MB cells generated tumoroids in the presence of control astrocytes (Fig. 4o). However, the number of tumoroids was significantly reduced in cultures including Shh-deficient astrocytes (Fig. 4p–r), confirming that astrocytes-generated Shh is required for the formation of MB tumoroids.

Despite the reduced number, tumoroids in MB cell monocultures exhibited comparable cytoarchitecture with those from the coculture of MB cells and astrocytes (supplementary Fig. S6A-6B, and Fig. 5a–c). Of note, the few tumoroids showed extensive presence of Nestin (supplementary Fig. S6C-6D). Moreover, Hh pathway was found activated in those tumoroids harvested from the culture of MB cell alone (supplementary Fig. S6E-6F). Hence, we went back and questioned whether astrocyte "contaminants" were responsible for the few intact tumoroids found in the alleged monocultures. Indeed, the few remaining tumoroids contained astrocytes (S100β+) (supplementary S6G-6H), which explains the observed sustained Hh signaling and the effective tumoroid formation. Whether the "contaminants" were indeed astrocytes that remained from an imperfect cell sorting or whether trans differentiation took place [36], remains to be tested.

Astrocyte-derived ECM supports MB tumoroid formation

Besides Shh secretion, astrocytes were considered as a source for ECM that is known to be critical for brain development and regeneration [37, 38]. We therefore examined whether astrocytes-derived ECM supports MB tumoroid formation. Fibrous fibronectin, a component of mesenchymal ECM [39, 40], was detected in MB tumoroids (Fig. 5a–c). To examine the role of astrocytes-derived ECM in MB tumoroid formation, we purified astrocytes from mouse cerebella at postnatal day 2 by FACS using an antibody against ACSA2. After 7 days in culture, astrocytes expressing GFAP extended long processes, and produced ECMs enriched with fibronectin (Fig. 5d, e). Further, acellular astrocyte-derived ECM was obtained by removing the astrocytes from a week old culture that was treated with ascorbic acid (Fig. 5f), following our established protocol [18]. We plated MB cells into these astrocyte-generated ECMs and cultured cells for 3 days. As a control, MB cells were cultured on PDL-coated coverslips. The proliferation of MB cells was examined by BrdU incorporation. As

shown in Fig. 5g, <10% of MB cells were BrdU positive after being cultured adherently. However, the proliferation of MB cells on astrocyte-derived ECM was significantly enhanced (Fig. 5h, i). These data suggest that astrocytes-derived ECM indeed supports MB cell proliferation. In addition, MB cells cultured on the ECM were treated with DMSO or 100 nM vismodegib for 3 days. Compared with DMSO, vismodegib significantly repressed ECM-induced MB cell proliferation (Fig. 5j, k), resulting in a decreased percentage of BrdU+ cells in the culture (Fig. 5l). These data suggest that Hh pathway was activated in MB cells cultured on astrocyte-derived ECM. In addition, we also prepared ECM from pancreatic fibroblasts, as previously described [19]. MB cells were plated on fibroblast-derived ECM for 2 days, and MB cell proliferation was assessed via indirect immunofluorescence. MB cells cultured on PDL-coated coverslips for 2 days were used as a control. As shown in supplementary Fig. S7, MB cell proliferation was significantly diminished in MB cells cultured on the fibroblast-derived ECM, compared with that of the adherent MB culture. Results suggest that the supportive role of ECM seen in MB cell proliferation is attained by astrocytes, but not by fibroblast-derived ECMs, known to provide proliferative advantage to pancreatic (and other) cancer cells [41, 42].

To determine whether astrocytic Shh is retained/stored in the acellular astrocyte-derived ECM, we plated MB cells on the ECM or PDL-coated coverslips and treated with 1% 5E1 supernatant obtained from a mouse hybridoma to neutralize the Hh ligand [43]. As controls, the cell cultures were treated with 1% NS1 conditioned medium or 1% an isotype hybridoma supernatant (mouse IgG1). MB cell proliferation was examined by EdU incorporation assay. As shown in the supplementary Fig. S8A-D, no alterations in the proliferation of MB cells cultured on PDL-coated coverslips were observed in response to 5E1 treatment, compared with controls. However, 5E1 significantly inhibited the proliferation of MB cells cultured on astrocyte-derived ECMs, with no repression on the proliferation of MB cells following treatment with NS1 conditioned medium or with the isotype supernatant (supplementary Fig. S8E-I). These data suggest that ECM from astrocytes supports MB cell proliferation at least partially via Shh ligand. In addition, we examined the ability of astrocytes deficient in Shh to form ECM. As shown in the supplementary Fig. S9, Shh deletion significantly reduced the number of astrocytes in the culture (supplementary Fig. S9A-B). We hence matched the numbers of plated astrocytes and examined ECM formation. Control astrocytes formed the ECM as expected, whereas the abundance of fibronectin and fibrous collagen was markedly reduced in ECMs deposited by Shh-deficient astrocytes (supplementary Fig. S9C–G), suggesting that Shh deletion significantly compromised the ability of
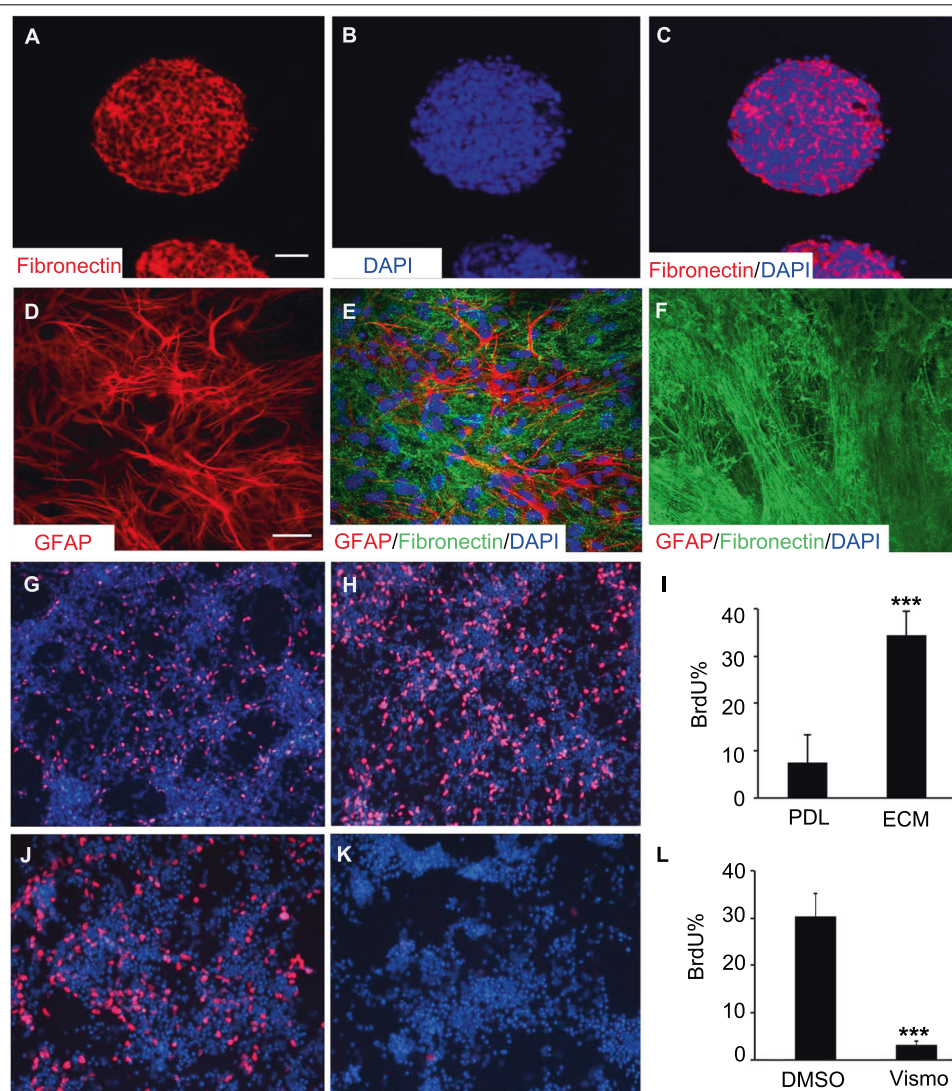
Fig. 5 Astrocyte-derived ECM supports MB cell proliferation. a–c MB tumoroids were examined for fibronectin content (**a**) by indirect immunofluorescence, and counterstained for nuclei using DAPI (**b**). A merged image of fibronectin and DAPI staining (**c**). **d–f** Astrocytes cultured for 3 days and treated with ascorbic acid ate (to stabilize ECM production) were immunostained for GFAP (**d**) and fibronectin (**e**) prior to cell extraction, as well as following cell extraction (**f**). Note that astrocytes (GFAP+) were successfully removed following the cell extraction, leaving astrocyte-derived ECM intact. **g–i** MB cells were adherently cultured on PDL-coated coverslips (**g**) or into astrocyte-derived ECM (**h**) for 3 days. MB cell culture was pulsed with BrdU for 2 h prior to the indirect immunofluorescence. Percentages of BrdU+ cells in MB cells on PDL or ECM were quantified (**i**). **j–l** MB cells cultured on astrocytes-derived ECM were treated with DMSO (**j**) or vismodegib (100 nM) (**k**) for 3 days together with pulsed-labeling of BrdU for 2 h before being collected for immunocytochemistry. Percentages of BrdU+ cells in cultured MB cells were quantified (**l**). Scale bar: 50 μm (**a–c**), 100 μm (**d–f**, **g–h**, and **j–k**).

astrocytes to produce ECM. Collectively, these data imply that astrocytic Shh plays an important role in astrocyte's ability to form tumor-promoting ECMs.

We next turned our attention to the astrocyte-derived ECM. Integrin β1 subfamily constitutes a major class of integrin heterodimers that mediate cell interactions with ECM proteins like collagen and fibronectin [12]. For example, α5β1-integrin constitutes the main fibronectin receptor, the extended αv-integrin subfamily is a major cell-ECM receptor that includes fibronectin but also multiple additional ECM protein ligands [12]. To further examine whether ECM proteins, such as collagen and fibronectin, are important in supporting MB cell proliferation, we treated MB cells with functionally blocking antibodies against integrins β1, α5β1 or αv, and proceeded to plating these into astrocyte-derived acellular ECM, as before [19]. As shown in supplementary Fig. S10, the inhibition of all the tested types of integrins significantly repressed the observed ECM-induced MB cell proliferation. These data suggest that fibronectin and collagen, among others, in astrocyte-derived ECM are required for supporting MB cell proliferation.
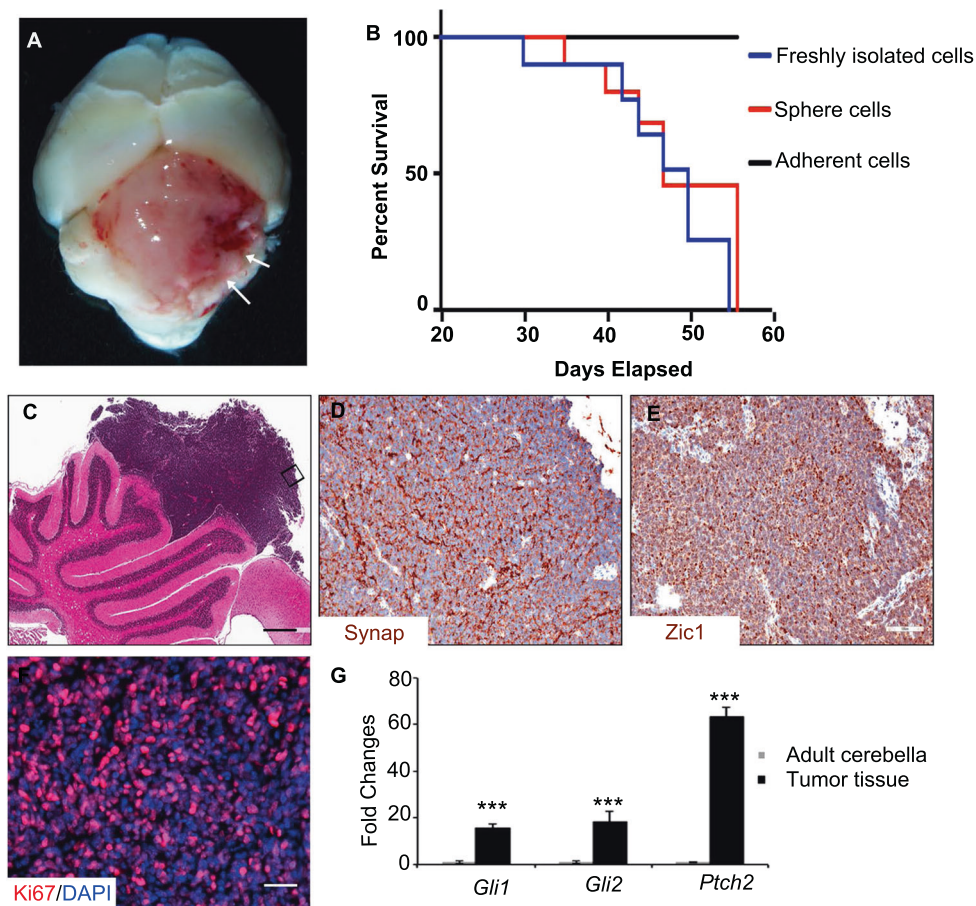
Fig. 6 MB cells in tumoroids retain the tumorigenic potential. a, b Cells dissociated from tumoroids developed into a tumor in the cerebellum of *CB17/SCID* mouse (pointed by arrows) upon intracranial transplantation (**a**). Survival curves of *CB17/SCID* mice following transplantation of freshly isolated cells ($n = 6$, median survival: 50ds), tumoroid cells ($n = 6$, median survival: 47ds) or MB cells harvested from adherent culture ($n = 7$) (**b**). **c–f** HE staining of the recipient cerebellum transplanted with tumoroid cells (**c**), and synaptophysin (Synap, **d**) as well as Zic1 expression (**e**) as seen in the tumor tissue examined by immunohistochemistry. Images in (**d**) and (**e**) correlate to the box region in (**c**). Frozen cerebellar sections from *CB17/SCID* mice transplanted with tumoroid cells were immunostained for Ki67 (**f**). DAPI was used to counterstain cell nuclei. **g** Expression of *Gli1*, *Gli2*, and *Ptch2* mRNAs in adult cerebella from *CB17/SCID* mice and tumor tissues from *CB17/SCID* mice transplanted with tumoroid cells, examined by q-PCR. Scale bars: 100 μm (**c**), 50 μm (**d–f**).

MB cells in tumoroids retain the tumorigenicity

The above findings revealed that tumor cells sustain their proliferation and Hh signaling in tumoroids. We next examined whether the tumorigenicity of MB cells is sustained in tumoroids. Cells dissociated from MB tumoroids were transplanted intracranially into the cerebella of *CB17/SCID* mice as previously described [6]. As controls, MB cells freshly isolated from *Math1-Cre/Ptch1^fl/fl^* mice, as well as MB cells adherently cultured for 4 days were also transplanted into *CB17/SCID* mice. Cells from the three-dimensional tumoroids effectively developed into tumors in the cerebella of *CB17/SCID* mice following the transplantation (Fig. 6a). As expected, freshly isolated MB cells also formed tumors with 100% penetrance. However, no tumors were detected if adherently cultured MB cells were used, suggesting that the tumorigenicity of MB cells was compromised after being cultured adherently. Medium survival of *CB17/SCID* mice transplanted with tumoroid-derived cells was comparable to that of freshly isolated tumor cells. These data indicate that the tumorigenicity of MB cells is not affected by in vitro tumoroids culture.

We further characterized tumors formed from cells harvested from MB tumoroids. As shown in Fig. 6c, tumor cells with condensed nuclei and sparse cytoplasm were found in the recipient cerebellum of *CB17/SCID* mice. Tumor cells expressed high levels of synaptophysin (Fig. 6d) and Zic1 (Fig. 6e), and were highly proliferative with Ki67 expression in the majority of tumor cells (Fig. 6f), which are established characteristics for MB cells [44]. In addition, we harvested tumor tissues from recipient cerebella to examine Hh signaling by q-PCR. Adult cerebella from *CB17/SCID* mice were also collected as a control. As shown in Fig. 6g, expression levels of *Gli1*, *Gli2*,

and *Ptch2* were markedly elevated in the tumor tissue compared with those in control cerebella, indicating that Hh pathway was activated in tumor cells developed in *CB17/SCID* mice. These data confirm that MB cells from ex vivo tumoroids effectively sustain a tumorigenic potential.

Discussion

Established cell lines are widely utilized in cancer research, in that they are readily available, easy to propagate or preserve, and could be used for high-throughput assays [45]. However, the long-term culture of primary cancer cells often causes genetic alterations and/or changes in cell phenotypes and functions. As a result, these cells may not always be capable of recapitulating transcriptional and phenotypic features of cancer cells in vivo. The progress in the basic research and preclinical studies of MB is greatly impeded by the lack of reliable cell lines. Genetically engineered mouse (GEM) models have been utilized to study MB, since these mice develop tumors resembling human MB. However, MB cells isolated from the above alluded GEM models cannot be cultured for long-term studies or preserved ex vivo, because tumor cells often undergo terminal differentiation in adherent cultures. Therefore, investigators are often burdened by the need of freshly isolating MB cells from GEM models. Here we demonstrate that MB cells from both mice and human origins can form long-term proliferative tumoroids in vitro. More importantly, such tumoroids can be passaged and cryopreserved without alterations in the proliferation of MB cells and the constitutive activation of Hh pathway. In addition, MB cells from such tumoroids effectively developed tumors in immunodeficient mice upon intracranial transplantation, indicating that the tumorigenicity of those MB cells is not compromised by this in vitro three-dimensional culturing approach.

Ptch1 deficient mice are often used in studying Hh-MB, since these mice develop desmoplastic MB in their cerebella and they harbored an activated Hh pathway. However, Hh pathway is rapidly suppressed in these MB cells upon being cultured adherently [15, 16]. Due to the repressed Hh pathway, adherent MB cells permanently ceased dividing and lost their tumorigenicity. Here we found that MB cells in tumoroids maintain the elevated expression levels of *Gli1*, *Ptch2*, and *Sfrp1*, suggesting that Hh signaling is preserved in tumor cells. Moreover, vismodegib can suppress tumoroids formation of MB cells, indicating that Hh signaling is sustained in tumoroids. Therefore, tumoroid culture could be utilized to study the Hh signaling in MB cells, which is consistent with a recent report [46].

We further demonstrate that astrocytes, the main stromal components of MB, can support tumoroids formation of MB cells, in that tumoroid-forming capacity of MB cells was dramatically enhanced in the presence of astrocytes and compromised in the absence of these stromal cells. Astrocytes highly express Shh gene, and deletion of *Shh* gene in astrocytes significantly inhibited MB tumoroid formation. These results indicate that astrocytic Shh plays an important role in stimulating MB cells to form tumoroids. Future studies are warranted to identify the receptor(s) for Shh ligand in *Ptch1*-deficient MB cells. In addition, our studies reveal that astrocytes support MB cell proliferation through the provision of stromal ECM. The role of astrocyte-derived ECM is not limited to the provision of physical scaffold, in that the proliferation of MB cell was not enhanced (even inhibited) by fibroblast-derived ECM. The proliferation of MB cells on astrocyte-derived ECM was repressed by the Shh neutralizing antibody, 5E1, suggesting that Shh ligand contributes to the increased proliferation of MB cells on astrocyte-derived ECM. Disrupted interaction between tumor cells and ECM proteins like fibronectin and collagen by the blockage of integrins on MB cells, significantly repressed the observed tumor cell proliferation induced by astrocytes-derived ECM. These findings suggest that besides Shh, fibronectin, collagen and potentially other ECM proteins are involved in supporting MB cell proliferation. It is also possible that other growth factors and/or cytokines in the astrocyte-derived ECM may also play a role in stimulating the proliferation and Hh signaling in MB cells.

In our studies, we established that NB-B27 plus 1% serum represents the optimal culture medium for supporting MB tumoroid formation. Tumoroids forming conditions were previously utilized to study tumor progression as well as the biology of cancer stem cells in MB [47–49]. bFGF and EGF were often added into the culture medium in the previous studies, although bFGF was identified as a potent inhibitor of Hh pathway in MB cells [50]. Both EGF and bFGF are necessary for the self-renewal of stem cell populations, which may not be ideal for the proliferation of bulk tumor cells as well as long-term Hh pathway activation. In our studies, the addition of EGF and bFGF in the culture medium was dispensable for attaining effective MB tumoroids formation.

It has been demonstrated that cells cultured as monolayers on flat surfaces, do not faithfully simulate in vivo conditions because the tissue architecture and cell–cell contact are greatly altered in such two dimensional systems [51]. Three-dimensional cultures are well documented to regain key intrinsic properties and to better mimicking the in vivo niche [52]. In our studies, we demonstrate that MB tumoroids contain stromal cells and ECM, both known to be essential components needed for recapitulating in vivo-like tumor cell behaviors [52]. Previous studies also revealed that proliferating, quiescent, and dying cells coexist in

normoxic, hypoxic, or necrotic zones within spheroids, resembling the conditions seen in human tumor masses [53]. Therefore, tumoroid cultures that incorporate tumor and stromal cells as well as stromal ECM, like the ones presented in this study, represent an ideal new three-dimensional model system that could accelerate research of MB including the development of novel strategies to treat this devastating disease.

Compliance with ethical standards

Conflict of interest The authors declare that they have no conflict of interest.

Publisher's note Springer Nature remains neutral with regard to jurisdictional claims in published maps and institutional affiliations.

References

1. Lee RT, Zhao Z, Ingham PW. Hedgehog signalling. Development. 2016;143:367–72.
2. Ingham PW, McMahon AP. Hedgehog signaling in animal development: paradigms and principles. Genes Dev. 2001;15:3059–87.
3. Rohatgi R, Milenkovic L, Corcoran RB, Scott MP. Hedgehog signal transduction by Smoothened: pharmacologic evidence for a 2-step activation process. Proc Natl Acad Sci USA. 2009;106:3196–201.
4. Northcott PA, Korshunov A, Pfister SM, Taylor MD. The clinical implications of medulloblastoma subgroups. Nat Rev Neurol. 2012;8:340–51.
5. Liu Y, Yuelling LW, Wang Y, Du F, Gordon RE, O'Brien JA, et al. Astrocytes promote medulloblastoma progression through hedgehog secretion. Cancer Res. 2017;77:6692–703.
6. Li P, Lee EH, Du F, Gordon RE, Yuelling LW, Liu Y, et al. Nestin mediates hedgehog pathway tumorigenesis. Cancer Res. 2016;76:5573–83.
7. Yauch RL, Gould SE, Scales SJ, Tang T, Tian H, Ahn CP, et al. A paracrine requirement for hedgehog signalling in cancer. Nature. 2008;455:406–10.
8. Tian C, Clauser KR, Ohlund D, Rickelt S, Huang Y, Gupta M, et al. Proteomic analyses of ECM during pancreatic ductal adenocarcinoma progression reveal different contributions by tumor and stromal cells. Proc Natl Acad Sci USA. 2019;116:19609–18.
9. Frantz C, Stewart KM, Weaver VM. The extracellular matrix at a glance. J Cell Sci. 2010;123(Pt 24):4195–200.
10. Lu P, Weaver VM, Werb Z. The extracellular matrix: a dynamic niche in cancer progression. J Cell Biol. 2012;196:395–406.
11. Hamidi H, Ivaska J. Every step of the way: integrins in cancer progression and metastasis. Nature Rev Cancer. 2018;18:533–48.
12. Hynes RO. Integrins: bidirectional, allosteric signaling machines. Cell. 2002;110:673–87.
13. Goodrich LV, Milenkovic L, Higgins KM, Scott MP. Altered neural cell fates and medulloblastoma in mouse patched mutants. Science. 1997;277:1109–13.
14. Yang ZJ, Ellis T, Markant SL, Read TA, Kessler JD, Bourboulas M, et al. Medulloblastoma can be initiated by deletion of Patched in lineage-restricted progenitors or stem cells. Cancer Cell. 2008;14:135–45.
15. Curran T. Reproducibility of academic preclinical translational research: lessons from the development of Hedgehog pathway inhibitors to treat cancer. Open Biol. 2018;8:180098.
16. Sasai K, Romer JT, Lee Y, Finkelstein D, Fuller C, McKinnon PJ, et al. Shh pathway activity is down-regulated in cultured medulloblastoma cells: implications for preclinical studies. Cancer Res. 2006;66:4215–22.
17. Du F, Yuelling L, Lee EH, Wang Y, Liao S, Cheng Y, et al. Leukotriene synthesis is critical for medulloblastoma progression. Clinical Cancer Res. 2019;25:6475–86.
18. Franco-Barraza J, Beacham DA, Amatangelo MD, Cukierman E. Preparation of extracellular matrices produced by cultured and primary fibroblasts. Curr Protoc Cell Biol. 2016;71:10.9.1–34.
19. Franco-Barraza J, Francescone R, Luong T, Shah N, Madhani R, Cukierman G, et al. Matrix-regulated integrin αvβ5 maintains α5β1-dependent desmoplastic traits prognostic of neoplastic recurrence. Elife. 2017;6:e20600.
20. Gordon RE, Zhang L, Peri S, Kuo YM, Du F, Egleston BL, et al. Statins synergize with hedgehog pathway inhibitors for treatment of medulloblastoma. Clinical Cancer Res. 2018;24:1375–88.
21. Izant JG, McIntosh JR. Microtubule-associated proteins: a monoclonal antibody to MAP2 binds to differentiated neurons. Proc Natl Acad Sci USA. 1980;77:4741–5.
22. Katsetos CD, Frankfurter A, Christakos S, Mancall EL, Vlachos IN, Urich H. Differential localization of class III, beta-tubulin isotype and calbindin-D28k defines distinct neuronal types in the developing human cerebellar cortex. J Neuropathol Exp Neurol. 1993;52:655–66.
23. Ellis T, Smyth I, Riley E, Graham S, Elliot K, Narang M, et al. Patched 1 conditional null allele in mice. Genesis. 2003;36:158–61.
24. Hubert CG, Rivera M, Spangler LC, Wu Q, Mack SC, Prager BC, et al. A three-dimensional organoid culture system derived from human glioblastomas recapitulates the hypoxic gradients and cancer stem cell heterogeneity of tumors found in vivo. Cancer Res. 2016;76:2465–77.
25. Karthaus WR, Iaquinta PJ, Drost J, Gracanin A, van Boxtel R, Wongvipat J, et al. Identification of multipotent luminal progenitor cells in human prostate organoid cultures. Cell. 2014;159:163–75.
26. Bardy C, van den Hurk M, Eames T, Marchand C, Hernandez RV, Kellogg M, et al. Neuronal medium that supports basic synaptic functions and activity of human neurons in vitro. Proc Natl Acad Sci USA. 2015;112:E2725–34.
27. Yokota N, Aruga J, Takai S, Yamada K, Hamazaki M, Iwase T, et al. Predominant expression of human zic in cerebellar granule cell lineage and medulloblastoma. Cancer Res. 1996;56:377–83.
28. Reynolds BA, Weiss S. Generation of neurons and astrocytes from isolated cells of the adult mammalian central nervous system. Science. 1992;255:1707–10.
29. Mao X, Fujiwara Y, Chapdelaine A, Yang H, Orkin SH. Activation of EGFP expression by Cre-mediated excision in a new ROSA26 reporter mouse strain. Blood. 2001;97:324–6.

30. Rudin CM, Hann CL, Laterra J, Yauch RL, Callahan CA, Fu L, et al. Treatment of medulloblastoma with hedgehog pathway inhibitor GDC-0449. New Engl J Med. 2009;361:1173–8.

31. Kurtz A, Zimmer A, Schnutgen F, Bruning G, Spener F, Muller T. The expression pattern of a novel gene encoding brain-fatty acid binding protein correlates with neuronal and glial cell development. Development. 1994;120:2637–49.

32. Garcia AD, Doan NB, Imura T, Bush TG, Sofroniew MV. GFAP-expressing progenitors are the principal source of constitutive neurogenesis in adult mouse forebrain. Nat Neurosci. 2004;7: 1233–41.

33. Yokota N, Mainprize TG, Taylor MD, Kohata T, Loreto M, Ueda S, et al. Identification of differentially expressed and developmentally regulated genes in medulloblastoma using suppression subtraction hybridization. Oncogene. 2004;23:3444–53.

34. Chen JK, Taipale J, Cooper MK, Beachy PA. Inhibition of Hedgehog signaling by direct binding of cyclopamine to Smoothened. Genes Dev. 2002;16:2743–8.

35. Platt RJ, Chen S, Zhou Y, Yim MJ, Swiech L, Kempton HR, et al. CRISPR-Cas9 knockin mice for genome editing and cancer modeling. Cell. 2014;159:440–55.

36. Yao M, Ventura PB, Jiang Y, Rodriguez FJ, Wang L, Perry JSA, et al. Astrocytic trans-differentiation completes a multicellular paracrine feedback loop required for medulloblastoma tumor growth. Cell. 2020;180:502–20. e19.

37. Molofsky AV, Krencik R, Ullian EM, Tsai HH, Deneen B, Richardson WD, et al. Astrocytes and disease: a neurodevelopmental perspective. Genes Dev. 2012;26:891–907.

38. Wiese S, Karus M, Faissner A. Astrocytes as a source for extracellular matrix molecules and cytokines. Front Pharmacol. 2012;3:120.

39. Yamada KM, Yamada SS, Pastan I. Cell surface protein partially restores morphology, adhesiveness, and contact inhibition of movement to transformed fibroblasts. Proc Natl Acad Sci USA. 1976;73:1217–21.

40. Ali IU, Mautner V, Lanza R, Hynes RO. Restoration of normal morphology, adhesion and cytoskeleton in transformed cells by addition of a transformation-sensitive surface protein. Cell. 1977;11:115–26.

41. Castello-Cros R, Khan DR, Simons J, Valianou M, Cukierman E. Staged stromal extracellular 3D matrices differentially regulate breast cancer cell responses through PI3K and beta1-integrins. BMC Cancer. 2009;9:94.

42. Malik R, Luong T, Cao X, Han B, Shah N, Franco-Barraza J, et al. Rigidity controls human desmoplastic matrix anisotropy to enable pancreatic cancer cell spread via extracellular signal-regulated kinase 2. Matrix Biol. 2019;81:50–69.

43. Ericson J, Morton S, Kawakami A, Roelink H, Jessell TM. Two critical periods of Sonic Hedgehog signaling required for the specification of motor neuron identity. Cell. 1996;87:661–73.

44. Borowska A, Jozwiak J. Medulloblastoma: molecular pathways and histopathological classification. Arch Med Sci. 2016;12: 659–66.

45. Wilding JL, Bodmer WF. Cancer cell lines for drug discovery and development. Cancer Res. 2014;74:2377–84.

46. Petroni M, Sahun Roncero M, Ramponi V, Fabretti F, Nicolis Di Robilant V, Moretti M, et al. SMO-M2 mutation does not support cell-autonomous Hedgehog activity in cerebellar granule cell precursors. Sci Rep. 2019;9:19623.

47. Zhao X, Ponomaryov T, Ornell KJ, Zhou P, Dabral SK, Pak E, et al. RAS/MAPK activation drives resistance to smo inhibition, metastasis, and tumor evolution in shh pathway-dependent tumors. Cancer Res. 2015;75:3623–35.

48. Ward RJ, Lee L, Graham K, Satkunendran T, Yoshikawa K, Ling E, et al. Multipotent CD15+ cancer stem cells in patched-1-deficient mouse medulloblastoma. Cancer Res. 2009;69:4682–90.

49. Heil C. Hedgehog pathway permissive conditions allow generation of immortal cell lines from granule cells derived from cancerous and non-cancerous cerebellum. Open Biol. 2019;9:180145.

50. Fogarty MP, Emmenegger BA, Grasfeder LL, Oliver TG, Wechsler-Reya RJ. Fibroblast growth factor blocks Sonic hedgehog signaling in neuronal precursors and tumor cells. Proc Natl Acad Sci USA. 2007;104:2973–8.

51. Cukierman E, Pankov R, Stevens DR, Yamada KM. Taking cell-matrix adhesions to the third dimension. Science. 2001;294: 1708–12.

52. Yamada KM, Cukierman E. Modeling tissue morphogenesis and cancer in 3D. Cell. 2007;130:601–10.

53. Hirschhaeuser F, Menne H, Dittfeld C, West J, Mueller-Klieser W, Kunz-Schughart LA. Multicellular tumor spheroids: an underestimated tool is catching up again. J Biotechnol. 2010;148: 3–15.